

Effect of Raman-pulse duration related to the magnetic field gradient in high-precision atom gravimeters

Yuan Cheng(程源), Yu-Jie Tan(谈玉杰), Min-Kang Zhou(周敏康), Xiao-Chun Duan(段小春), Cheng-Gang Shao(邵成刚), Zhong-Kun Hu(胡忠坤)
Citation: Chin. Phys. B . 2018, 27(3): 030303. **doi:** 10.1088/1674-1056/27/3/030303

Journal homepage: http://cpb.iphy.ac.cn; http://iopscience.iop.org/cpb

What follows is a list of articles you may be interested in

Comparison of the sensitivities for atom interferometers in two different operation methods

Xiao-Chun Duan(段小春), De-Kai Mao(毛德凯), Xiao-Bing Deng(邓小兵), Min-Kang Zhou(周敏康), Cheng-Gang Shao(邵成刚), Zhu Zhu(祝竺), Zhong-Kun Hu(胡忠坤)
Chin. Phys. B . 2018, 27(1): 013701. **doi:** 10.1088/1674-1056/27/1/013701

Common-mode noise rejection using fringe-locking method in WEP test by simultaneous dual-species atom interferometers

Xiao-Bing Deng(邓小兵), Xiao-Chun Duan(段小春), De-Kai Mao(毛德凯), Min-Kang Zhou(周敏康), Cheng-Gang Shao(邵成刚), Zhong-Kun Hu(胡忠坤)
Chin. Phys. B . 2017, 26(4): 043702. **doi:** 10.1088/1674-1056/26/4/043702

Investigation of the thermal adaptability for a mobile cold atom gravimeter

Qi-Yu Wang(王启宇), Zhao-Ying Wang(王兆英), Zhi-Jie Fu(付志杰), Qiang Lin(林强)
Chin. Phys. B . 2016, 25(12): 123701. **doi:** 10.1088/1674-1056/25/12/123701

Rapid extraction of the phase shift of the cold-atom interferometer via phase demodulation

Cheng Bing, Wang Zhao-Ying, Xu Ao-Peng, Wang Qi-Yu, Lin Qiang
Chin. Phys. B . 2015, 24(11): 113704. **doi:** 10.1088/1674-1056/24/11/113704

Precision measurement with atom interferometry

Wang Jin
Chin. Phys. B . 2015, 24(5): 053702. **doi:** 10.1088/1674-1056/24/5/053702

Effect of Raman-pulse duration related to the magnetic field gradient in high-precision atom gravimeters*

Yuan Cheng(程源), Yu-Jie Tan(谈玉杰)†, Min-Kang Zhou(周敏康),
Xiao-Chun Duan(段小春), Cheng-Gang Shao(邵成刚), and Zhong-Kun Hu(胡忠坤)‡

MOE Key Laboratory of Fundamental Physical Quantities Measurements, Hubei Key Laboratory of Gravitation and Quantum Physics, School of Physics, Huazhong University of Science and Technology, Wuhan 430074, *China*

(Received 19 September 2017; revised manuscript received 3 December 2017; published online 11 February 2018)

The effect of the Raman-pulse duration related to the magnetic field gradient, as a systematic error, is playing an important role on evaluating the performance of high-precision atomic gravimeters. We study this effect with a simplified theoretical model of the time-propagation operator. According to the typical parameters, we find that this effect should be taken into account when the gravimeter reaches an accuracy of $10^{-10}g$, and the larger the pulse duration is, the more obvious the systematic effect will be. Finally, we make a simple discussion on the possibility of testing this effect.

Keywords: atom gravimeters, magnetic field gradient, Raman-pulse duration, time-propagation operator

PACS: 03.75.Dg, 37.25.+k, 32.60.+i **DOI:** 10.1088/1674-1056/27/3/030303

1. Introduction

Since the atom interferometer was first demonstrated in 1991,[1] this technology has been developed rapidly and highly sensitive instruments have been realized. It has been applied to many precision measurements,[2] such as measurements of local gravity g[3–7] and its gradients,[8–10] the fine-structure constant α,[11–13] the Sagnac effect,[14–16] Newton's gravitational constant G,[17,18] the weak equivalence principle,[19–24] and even for searching gravitational waves.[25,26] Recently, the atom interferometer has been utilized to precisely measure the map of a magnetic field[27,28] and the quadratic Zeeman coefficient.[29,30] The sensitivity of an atom interferometer linearly scales with the space–time area enclosed by the matter waves.[31] Researchers are struggling to achieve ambitious high-precision measurements through producing large-momentum-transfer atom optics[32–36] and a long coherence time.[37–39] For instance, Kasevich's group[40] has achieved a light-pulse atom interferometer with wave packets separated by up to 54 cm on a timescale of 1 s. Precision measurements of g are of interest in a wide range of applications in geophysics,[41] inertial navigation,[42] and fundamental research.[43] For high-precision gravity measurements,[44] the atom gravimeters have achieved an accuracy of a few μGal (1 μGal $= 10^{-9}g$),[3,4] which are able to obtain the absolute gravity value directly referenced to atomic standards. However, the ultimate accuracy of the measurement still depends on the understanding of the potential systematic errors.

In the mature atom interferometer, some significant systematic errors have been considered, such as the AC stark effect,[1,45–48] quadratic Zeeman effect,[49–53] gravity gradient effect,[3,54] and some other effects.[55–62] As the atom interferometer is rapidly developed, more and more schemes are proposed to test general relativity with atom interferometry, in which a lot of minor systematic effects should be taken into account, such as the Raman-pulse-duration effect related to the gravitational field[63–67] and the Raman-pulse-duration effect related to the inhomogeneous magnetic field. In the past few years, the Raman-pulse-duration effect related to the gravitational field has been studied extensively, while the Raman-pulse-duration effect related to the inhomogeneous magnetic field has not been considered before. In this paper, we focus on analyzing the Raman-pulse-duration effect of atom gravimeters in an inhomogeneous magnetic field. During the gravity-measurement process, there are mainly two ingredients influencing the atomic propagation: the Earth's gravitational field and the laser field. Here, we use the time-propagation operator to describe the dynamic behavior of a two-level-atom system in the Schrödinger picture, where the time-propagation operator is decomposed into two parts for simplicity: the free-propagation part and the interaction part with the laser field. Based on this, we can derive the atomic wave function easily, and further calculate the coupling effect of the Raman-pulse duration and the magnetic field gradient, which has not been considered before. For the typical parameters, we find that this coupling effect must be taken into account when the expected accuracy of an atomic gravimeter reaches $10^{-10}g$.

The outline of this paper is as follows. In Section 2, we

*Project supported by the National Natural Science Foundation of China (Grant Nos. 11625417, 11727809, 11474115, 91636219, and 91636221) and the Post-doctoral Science Foundation of China (Grant No. 2017M620308).

†Corresponding author. E-mail: yjtan@hust.edu.cn

‡Corresponding author. E-mail: zkhu@hust.edu.cn

© 2018 Chinese Physical Society and IOP Publishing Ltd

describe the theoretical analytical framework, showing how the time-propagation operator is used to analyze the dynamic behavior of a two-level-atom system. In Section 3, we analyze the Raman-pulse-duration effect in an inhomogeneous magnetic field, and present the calculation for the coupling effect between the Raman-pulse duration and the magnetic field gradient in detail. In Section 4, we discuss the suppression of the coupling effect between the Raman-pulse duration and the magnetic field gradient, and how to test this coupling effect experimentally. Finally, the paper is concluded in Section 5.

2. Theoretical analytical frameworks

For a typical Raman atom interferometer, the Raman beams are formed by a pair of opposite propagation far-detuned laser beams, which are used to manipulate the atomic states. For the interaction of a three-level atom using short laser pulses, adiabatic elimination will produce an effective two-state system.[67] Based on the approximate two-level model, we study the coupling effect between the Raman-pulse duration and the magnetic field gradient, which has not been studied before. In the Schrödinger picture, for a two-level system with two hyperfine states $|g\rangle$ and $|e\rangle$, the atomic wave function $|\psi(t)\rangle$ can be described as

$$|\psi(t)\rangle = U(t)\,|\psi(0)\rangle\,, \tag{1}$$

with $U(t)$ the time-propagation operator,[67,68] which can be decomposed into two parts the atomic free-propagation operator $U_{\rm prop}(t)$ and the interaction operator $U_{\rm laser}(t)$ as

$$U(t) \equiv U_{\rm prop}(t)U_{\rm laser}(t). \tag{2}$$

This decomposition-operator method has been studied in our previous work.[67] Here, we use a similar method to analyze the effect of the Raman-pulse duration in the interferometer. Firstly, we analyze the time-propagation operator $U(t)$ in a typical Mach–Zehnder atom interferometer. In this configuration, the atoms are manipulated by a $\pi/2$–π–$\pi/2$ pulse sequence, which is used to split, reflect, and recombine the atomic wave packets, as shown in Fig. 1. The durations of the pulses are τ_1, τ_2, and τ_3, respectively, and the free-propagation time between the three pulses is T and T', respectively. When considering the pulse duration, the propagation operator $U_{\rm laser}(\tau)$ can be used to describe the instantaneous interaction of the atoms with the laser. $U_{\rm prop}(\tau)$ is the free-propagation operator during the finite pulse duration, which can be merged into the free-propagation operator $U_{\rm prop}(T)$ between pulses, resulting in a total free-propagation operator $U_{\rm prop}(\tau+T)$. Then, the time-propagation operator can be expressed as $U_{\rm laser}(\tau)$ and $U_{\rm prop}(\tau+T)$, in which the magnetic field gradient effect has been taken into account. Based on Eq. (1), the final wave function can be obtained. Finally, we can derive the interference phase containing the coupling effect of the Raman-pulse duration and the magnetic field gradient.

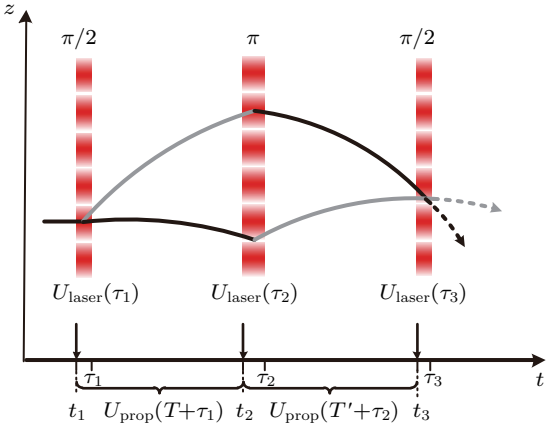


Fig. 1. (color online) Space–time diagram for the Mach–Zehnder type atom interferometry. The pulse durations of the $\pi/2$–π–$\pi/2$ sequences are τ_1, τ_2, and τ_3, respectively. The time of free propagation between the pulses is T and T', respectively. The time propagation operator $U(t)$ for an atom interferometer can be decomposed into five parts: $U_{\rm laser}(\tau_1)$, $U_{\rm prop}(T+\tau_1)$, $U_{\rm laser}(\tau_2)$, $U_{\rm prop}(T'+\tau_2)$, and $U_{\rm laser}(\tau_3)$.

3. Effect of Raman-pulse duration in an inhomogeneous magnetic field

The interaction between a two-level atomic system and an electromagnetic field can be described by Hamiltonian operator

$$\hat{H}(t) = \hbar\omega_g\,|g\rangle\langle g| + \hbar\omega_e\,|e\rangle\langle e| + \frac{\hat{\boldsymbol{p}}^2}{2m} + V(\boldsymbol{x}) - \boldsymbol{d}\cdot\boldsymbol{E}(t), \tag{3}$$

where $\hbar\omega_g$ and $\hbar\omega_e$ are respectively the internal energies of the ground and excited states, $\hat{\boldsymbol{p}}$ and $\boldsymbol{x}$ are respectively the atomic momentum and position operators, $V(\boldsymbol{x})$ represents any external potential acting on the center of mass motion, and $\boldsymbol{d}\cdot\boldsymbol{E}(t)$ describes the interaction between the atomic dipole moment $\boldsymbol{d}$ and the electric field $\boldsymbol{E}(t)$, which can be written as

$$-\boldsymbol{d}\cdot\boldsymbol{E}(t) = \hbar\Omega\cos\left[\omega_{\rm L}t - \boldsymbol{k}\cdot\boldsymbol{x} + \phi_{\rm L,0}\right]\begin{pmatrix}0 & 1\\ 1 & 0\end{pmatrix}, \tag{4}$$

with Rabi frequency

$$\Omega = -\boldsymbol{d}\cdot\boldsymbol{E}_0/\hbar, \tag{5}$$

where $\boldsymbol{E}_0$ is the amplitude of the electric field. In the atom interferometer, the moving atoms suffer from the external magnetic field in the vertical direction, which can induce the shift of the atomic energy levels. The interactive Hamiltonian between the atoms and magnetic field can be expressed as

$$H_B = \hbar\begin{pmatrix}1 & 0\\ 0 & -1\end{pmatrix}(\alpha_{\rm Z,I}B + \alpha_{\rm Z,II}B^2), \tag{6}$$

with $\alpha_{\rm Z,I}$ and $\alpha_{\rm Z,II}$ the typical parameters for ^{87}Rb atom. For a magnetic sensitive type interferometer, the first-order Zeeman parameter is $\alpha_{\rm Z,I} = 2\pi\times 0.7$ MHz/G, and the second-order

Zeeman parameter is $\alpha_{Z,II} = 2\pi \times 575.15$ Hz/G^2.[69] The inhomogeneous magnetic field can be written as

$$B(\boldsymbol{x}) \approx B_0 + \gamma_B \boldsymbol{x} \cdot \boldsymbol{e}_B, \tag{7}$$

where γ_B is the magnetic field gradient, and $\boldsymbol{e}_B$ is the direction of the magnetic field. To simplify the calculations, $\boldsymbol{g}_B$ can be defined as an equivalent gravitational field introduced by the magnetic field. We further define $\boldsymbol{g}_{B,i}$ with $i = \mathrm{I}, \mathrm{II}$ representing the first-order and the second-order Zeeman effects, respectively. Then the magnetic field gradient factor for the first-order Zeeman effect can be defined as

$$\boldsymbol{g}_{B,\mathrm{I}} = -\alpha_{Z,\mathrm{I}} \frac{\hbar \gamma_B}{m} \boldsymbol{e}_B. \tag{8}$$

Similar to the gravitational effect, the corresponding potential has a direct relation with the interference path. In the typical interferometer, the atoms are prepared in magnetic-field-insensitive states to avoid the first-order Zeeman effect. However, these states still show a second-order Zeeman shift in the inhomogeneous magnetic field. When neglecting the high-order effect of γ_B, we can obtain

$$\alpha_{Z,\mathrm{II}} B^2 \approx \alpha_{Z,\mathrm{II}} ({B_0}^2 + 2B_0 \gamma_B \boldsymbol{x} \cdot \boldsymbol{e}_B). \tag{9}$$

Similarly, the magnetic field gradient factor for the second-order Zeeman effect can be defined as

$$\boldsymbol{g}_{B,\mathrm{II}} = -\alpha_{Z,\mathrm{II}} \frac{2\hbar B_0 \gamma_B}{m} \boldsymbol{e}_B. \tag{10}$$

Then, equation (9) can be equivalently written as

$$\hbar \alpha_{Z,\mathrm{II}} B^2 \approx \hbar \alpha_{Z,\mathrm{II}} B_0^2 - m \boldsymbol{g}_{B,\mathrm{II}} \boldsymbol{x}. \tag{11}$$

For Eq. (11), the first term is independent of the interference path, not responsible for the systematic effect. Then, the interactive Hamiltonian between the atoms and magnetic field can be given by

$$H_B = -m \boldsymbol{g}_B \cdot \boldsymbol{x} \begin{pmatrix} 1 & 0 \\ 0 & -1 \end{pmatrix}. \tag{12}$$

The potential energy $V(\boldsymbol{x})$ induced by the uniform gravitational field and the inhomogeneous magnetic field can be written as

$$V(\boldsymbol{x}) = -m \boldsymbol{g} \cdot \boldsymbol{x} - m \boldsymbol{g}_B \cdot \boldsymbol{x} \begin{pmatrix} 1 & 0 \\ 0 & -1 \end{pmatrix}. \tag{13}$$

Based on Eqs. (3), (4), and (13), the Hamiltonian for a two-level atomic system in a uniform gravitational field and an inhomogeneous magnetic field can be written as

$$\hat{H} = \begin{pmatrix} E_e + \dfrac{\hat{\boldsymbol{p}}^2}{2m} - m(\boldsymbol{g} + \boldsymbol{g}_B) \cdot \boldsymbol{x} & 0 \\ 0 & E_g + \dfrac{\hat{\boldsymbol{p}}^2}{2m} - m(\boldsymbol{g} - \boldsymbol{g}_B) \cdot \boldsymbol{x} \end{pmatrix} + \frac{\hbar \Omega}{2} [\mathrm{e}^{\mathrm{i}(\omega_{\mathrm{L}} t - \boldsymbol{k} \cdot \boldsymbol{x} + \phi_{\mathrm{L},0})} + \mathrm{e}^{-\mathrm{i}(\omega_{\mathrm{L}} t - \boldsymbol{k} \cdot \boldsymbol{x} + \phi_{\mathrm{L},0})}] \begin{pmatrix} 0 & 1 \\ 1 & 0 \end{pmatrix}. \tag{14}$$

Through some simple calculations (see Appendix A), we can derive the unitary time-propagation operator $U(t)$ as

$$U(t) = \begin{pmatrix} \mathrm{e}^{-\mathrm{i}\beta_e t} & 0 \\ 0 & \mathrm{e}^{-\mathrm{i}\beta_g t} \end{pmatrix} \begin{pmatrix} \mathrm{e}^{-\mathrm{i}\eta(t)} & 0 \\ 0 & \mathrm{e}^{\mathrm{i}\eta(t)} \end{pmatrix} \times \begin{pmatrix} Y_{11}(\boldsymbol{p}_-) & Y_{12}(\boldsymbol{p}_-) \mathrm{e}^{\mathrm{i}\lambda} \\ Y_{21}(\boldsymbol{p}_+) \mathrm{e}^{-\mathrm{i}\lambda} & Y_{22}(\boldsymbol{p}_+) \end{pmatrix}, \tag{15}$$

with

$$\begin{aligned} \beta_e &= \omega_e + \frac{\hat{\boldsymbol{p}}^2}{2m\hbar} - \frac{m(\boldsymbol{g} + \boldsymbol{g}_B) \cdot \boldsymbol{x}}{\hbar}, \\ \beta_g &= \omega_g + \frac{\hat{\boldsymbol{p}}^2}{2m\hbar} - \frac{m(\boldsymbol{g} - \boldsymbol{g}_B) \cdot \boldsymbol{x}}{\hbar}, \\ \lambda &= \boldsymbol{k} \cdot \boldsymbol{x} - \phi_{\mathrm{L},0}, \eta(t) = \left[2\delta_0 t - (\alpha + \boldsymbol{k} \cdot \boldsymbol{g}) t^2\right]/4, \\ \delta_0 &= \omega_{\mathrm{L}} - \omega_{eg} - \boldsymbol{k} \cdot \hat{\boldsymbol{p}}/m - h\boldsymbol{k}^2/2m. \end{aligned} \tag{16}$$

Here, $\hat{\boldsymbol{p}}^2/2m - m(\boldsymbol{g} \pm \boldsymbol{g}_B) \cdot \boldsymbol{x}$ is the Hamiltonian of the center of mass, and α denotes the sweeping rate of lights' frequency, which is used to compensate the frequency shift induced by the Doppler effect for the moving atoms. More details can be found in Appendix A. To further simplify the calculations, $U(t)$ can be decomposed into two parts: the free propagation operator $U_{\mathrm{prop}}(t)$

$$U_{\mathrm{prop}}(t) = \begin{pmatrix} \mathrm{e}^{-\mathrm{i}\beta_e t} & 0 \\ 0 & \mathrm{e}^{-\mathrm{i}\beta_g t} \end{pmatrix}, \tag{17}$$

which describes the free propagation of the atoms, and the laser-propagation operator $U_{\mathrm{laser}}(t)$

$$U_{\mathrm{laser}}(t) = \begin{pmatrix} \mathrm{e}^{-\mathrm{i}\eta(t)} & 0 \\ 0 & \mathrm{e}^{\mathrm{i}\eta(t)} \end{pmatrix} \times \begin{pmatrix} Y_{11}(\boldsymbol{p}_-) & Y_{12}(\boldsymbol{p}_-) \mathrm{e}^{\mathrm{i}\lambda} \\ Y_{21}(\boldsymbol{p}_+) \mathrm{e}^{-\mathrm{i}\lambda} & Y_{22}(\boldsymbol{p}_+) \end{pmatrix}, \tag{18}$$

which describes the instantaneous interaction between the atoms and lasers. For a typical Mach–Zehnder atom interferometer, $\pi/2$ and π pulses are used to split and reflect the atomic wave packets, respectively, where the laser-propagation operator $U_{\mathrm{laser}}(t)$ can be respectively written as

$$U_{\pi/2}(t) = \frac{1}{\sqrt{2}} \begin{pmatrix} \mathrm{e}^{-\mathrm{i}\eta(t)} & 0 \\ 0 & \mathrm{e}^{\mathrm{i}\eta(t)} \end{pmatrix} \begin{pmatrix} \mathrm{e}^{\mathrm{i}\frac{4\eta(t)}{\pi}} & -\mathrm{i}\,\mathrm{e}^{\mathrm{i}\lambda} \\ -\mathrm{i}\,\mathrm{e}^{-\mathrm{i}\lambda} & \mathrm{e}^{-\mathrm{i}\frac{4\eta(t)}{\pi}} \end{pmatrix}, \tag{19}$$

$$U_{\pi}(t) = \begin{pmatrix} \mathrm{e}^{-\mathrm{i}\eta(t)} & 0 \\ 0 & \mathrm{e}^{\mathrm{i}\eta(t)} \end{pmatrix} \begin{pmatrix} 0 & -\mathrm{i}\,\mathrm{e}^{\mathrm{i}\lambda} \\ -\mathrm{i}\,\mathrm{e}^{-\mathrm{i}\lambda} & 0 \end{pmatrix}. \tag{20}$$

In this paper, we consider the plane wave approximation for the wave-packets of the atoms and assume that the atoms are initially in the state $|g\rangle$, which can be expressed by the wave function

$$\psi = \begin{pmatrix} \psi_e(t_1) \\ \psi_g(t_1) \end{pmatrix} = \begin{pmatrix} 0 \\ \mathrm{e}^{\mathrm{i}\boldsymbol{p} \cdot \boldsymbol{x}/\hbar} \end{pmatrix}, \tag{21}$$

with the starting time $t_1 = 0$. According to the timing diagram of the Raman-pulse sequences (see Fig. 1), the final wave function can be written as

$$\begin{pmatrix} \psi_e(t_3+\tau_3) \\ \psi_g(t_3+\tau_3) \end{pmatrix} = U_{\pi/2}(\tau_3)U_{\rm prop}(t_3-t_2)U_{\pi}(\tau_2)U_{\rm prop}(t_2)U_{\pi/2}(\tau_1)\begin{pmatrix} \psi_e(t_1) \\ \psi_g(t_1) \end{pmatrix}. \tag{22}$$

This transforming matrix between the initial and final wave functions is just like the optical propagation matrix. In this treatment, to obtain the final wave function, we just need the initial wave function and the propagation operator. With the specific free propagation operator and the laser propagation operator, the final wave function can be obtained as

$$\begin{pmatrix} \psi_e(t_3+\tau_3) \\ \psi_g(t_3+\tau_3) \end{pmatrix} = \begin{pmatrix} -\frac{\rm i}{2}\,{\rm e}^{\,{\rm i}(Z_{A_1}+Z_{B_1}+Z_{E_1}+\boldsymbol{k}_1\cdot\boldsymbol{x})} \\ -\frac{1}{2}\,{\rm e}^{\,{\rm i}(Z_{a_1}+Z_{B_1}+(\boldsymbol{k}_1-\boldsymbol{k})\boldsymbol{x}+Z_{E_1})} \end{pmatrix} + \begin{pmatrix} \frac{\rm i}{2}\,{\rm e}^{\,{\rm i}(Z_{A_2}+Z_{B_2}+Z_{E_2}+\boldsymbol{k}_2\cdot\boldsymbol{x})} \\ \frac{-1}{2}\,{\rm e}^{\,{\rm i}(Z_{a_2}+Z_{B_2}+(\boldsymbol{k}_2-\boldsymbol{k})\boldsymbol{x}+Z_{E_2})} \end{pmatrix}. \tag{23}$$

Finally, the interference phase can be obtained from the probability of atom in $|j\rangle$ state P_j ($j = g$ or e), based on the relation $\cos(\Delta\varphi_{\rm total}) = 2P_j - 1 = 2\left|\psi_j\right|^2 - 1$. When the atoms in $|e\rangle$ state are measured finally, the related interference phases are

$$\begin{aligned}
Z_{A_1} &= \left[-A(t_3,\tau_3)\left(1-\frac{4}{\pi}\right)+\frac{\boldsymbol{g}_B\cdot\boldsymbol{k}(t_3-2t_2)}{2}\tau_3\left(1-\frac{4}{\pi}\right)\right] \\
&\quad -\left[\phi_2+A(t_2,\tau_2)+\frac{\boldsymbol{g}_B\cdot\boldsymbol{k}}{2}t_2\tau_2\right], \\
Z_{A_2} &= -\left[\phi_3+A(t_3,\tau_3)+\frac{\boldsymbol{g}_B\cdot\boldsymbol{k}(t_3-2t_2)}{2}\tau_3\right] \\
&\quad +\left[\phi_2+A(t_2,\tau_2)-\frac{\boldsymbol{g}_B\cdot\boldsymbol{k}}{2}t_2\tau_2\right]-\phi_1, \\
Z_{B_1} &= -\int_0^{t_2} B_1\,{\rm d}t-\int_{t_2}^{t_3} B_2\,{\rm d}t, \\
Z_{B_2} &= -\int_0^{t_2} C_1\,{\rm d}t-\int_{t_2}^{t_3} C_2\,{\rm d}t, \\
Z_{E_1} &= \frac{\delta_0\tau_1}{2}\left(1-\frac{4}{\pi}\right),\quad Z_{E_2}=-\frac{\delta_0\tau_1}{2}, \\
\boldsymbol{k}_1 &= \frac{\boldsymbol{p}+\hbar\boldsymbol{k}+m\boldsymbol{g}t_3+m\boldsymbol{g}_B(t_3-2t_2)}{\hbar}, \\
\boldsymbol{k}_2 &= \frac{\boldsymbol{p}+\hbar\boldsymbol{k}+m\boldsymbol{g}t_3-m\boldsymbol{g}_B(t_3-2t_2)}{\hbar}.
\end{aligned} \tag{24}$$

While the related phases are

$$\begin{aligned}
Z_{a_1} &= \left[\phi_3+A(t_3,\tau_3)-\frac{\boldsymbol{g}_B\cdot\boldsymbol{k}(t_3-2t_2)}{2}\tau_3\right] \\
&\quad -\left[\phi_2+A(t_2,\tau_2)+\frac{\boldsymbol{g}_B\cdot\boldsymbol{k}}{2}t_2\tau_2\right], \\
Z_{a_2} &= \left[A(t_3,\tau_3)\left(1-\frac{4}{\pi}\right)+\frac{\boldsymbol{g}_B\cdot\boldsymbol{k}(t_3-2t_2)}{2}\tau_3\left(1-\frac{4}{\pi}\right)\right] \\
&\quad +\left[\phi_2+A(t_2,\tau_2)-\frac{\boldsymbol{g}_B\cdot\boldsymbol{k}}{2}t_2\tau_2\right]-\phi_1,
\end{aligned} \tag{25}$$

with

$$\begin{aligned}
A(t,\tau) &= \frac{\delta_0-(\alpha+\boldsymbol{k}\cdot\boldsymbol{g})t}{2}\tau, \\
B_1 &= \omega_g+\frac{|\boldsymbol{p}+m(\boldsymbol{g}-\boldsymbol{g}_B)t|^2}{2m\hbar}, \\
B_2 &= \omega_e+\frac{|\boldsymbol{p}+\hbar\boldsymbol{k}+m\boldsymbol{g}t+m\boldsymbol{g}_B(t-2t_2)|^2}{2m\hbar}, \\
C_1 &= \omega_e+\frac{|\boldsymbol{p}+\hbar\boldsymbol{k}+m(\boldsymbol{g}+\boldsymbol{g}_B)t|^2}{2m\hbar}, \\
C_2 &= \omega_g+\frac{|\boldsymbol{p}+m\boldsymbol{g}t-m\boldsymbol{g}_B(t-2t_2)|^2}{2m\hbar},
\end{aligned} \tag{26}$$

when the atoms in the $|g\rangle$ state are finally measured. In the atom interferometer, the interference phase is composed of three parts, atomic free-propagation phase shift $\Delta\varphi_{\rm prop}$, atomic instantaneous interactions with laser phase shift $\Delta\varphi_{\rm laser}$, and the observation position-dependent phase shift $\Delta\varphi_{\rm obs}$. By assuming that the atoms in the $|e\rangle$ state are measured, the total interference phase can be written as

$$\Delta\varphi_{\rm total} = \underbrace{(Z_{B_1}-Z_{B_2})}_{\Delta\varphi_{\rm prop}}+\underbrace{(Z_{A_1}+Z_{E_1})-(Z_{A_2}+Z_{E_2})}_{\Delta\varphi_{\rm laser}} +\underbrace{\boldsymbol{k}_1\cdot\boldsymbol{x}-\boldsymbol{k}_2\cdot\boldsymbol{x}}_{\Delta\varphi_{\rm obs}}. \tag{27}$$

Strictly, the evolution of atoms is the evolution of a Gauss wave packet. Arbitrary position $\boldsymbol{x}$ can be written as $\boldsymbol{x} = \boldsymbol{x}_{\rm cl} + \boldsymbol{x} - \boldsymbol{x}_{\rm cl}$, where $\boldsymbol{x}_{\rm cl}$ is the central position of the atoms. For the interference measurement we are concerned with, $\Delta\varphi_{\rm obs}$ can be rewritten as

$$\begin{aligned}
\Delta\varphi_{\rm obs} &= \boldsymbol{k}_1\cdot(\boldsymbol{x}_{\rm cl,upper}+\boldsymbol{x}-\boldsymbol{x}_{\rm cl,upper}) \\
&\quad -\boldsymbol{k}_2\cdot(\boldsymbol{x}_{\rm cl,lower}+\boldsymbol{x}-\boldsymbol{x}_{\rm cl,lower}) \\
&= (\boldsymbol{k}_1\cdot\boldsymbol{x}_{\rm cl,upper}-\boldsymbol{k}_2\cdot\boldsymbol{x}_{\rm cl,lower}) \\
&\quad +[\boldsymbol{k}_1\cdot(\boldsymbol{x}-\boldsymbol{x}_{\rm cl,upper})-\boldsymbol{k}_2\cdot(\boldsymbol{x}-\boldsymbol{x}_{\rm cl,lower})],
\end{aligned} \tag{28}$$

with $\boldsymbol{x}_{\rm cl,upper}$ ($\boldsymbol{x}_{\rm cl,lower}$) the classical position of the atoms in the upper (lower) path, and $\boldsymbol{x}$ the observation position, which can be chosen as $\boldsymbol{x} = (\boldsymbol{x}_{\rm cl,upper}+\boldsymbol{x}_{\rm cl,lower})/2 = \boldsymbol{v}_0 t_3 + \boldsymbol{g}t_3^2/2$. Usually, the first term in the above equation can be merged into the atomic free-propagation phase shift, and the last term is the separation phase shift. Here, the total interference phase contains the phase shift induced by the uniform gravitational field and the inhomogeneous magnetic field. We can decompose the total phase into two parts: $\Delta\varphi_g$ arising from the uniform gravitational field and $\Delta\varphi_B$ arising from the inhomogeneous magnetic field. According to Eqs. (24)–(27), the former can be written as

$$\Delta\varphi_g = \phi_{3,0}-2\phi_{2,0}+\phi_{1,0}-\delta_0\frac{\tau_2}{2}+\delta_0(t_3-2t_2)$$

$$-\frac{\alpha+\boldsymbol{k}\cdot\boldsymbol{g}}{2}(t_3^2-2t_2^2)$$
$$-\frac{\alpha+\boldsymbol{k}\cdot\boldsymbol{g}}{2}\left(t_3\tau_3\frac{4}{\pi}-2t_2\tau_2\right). \quad (29)$$

Assuming $\tau_2=2\tau_1=2\tau_3$, $t_3=2T+3\tau$, $t_2=T+\tau$ and neglecting the quadratic term of pulse duration τ, we can derive

$$\begin{aligned}\Delta\varphi_g &= \phi_{3,0}-2\phi_{2,0}+\phi_{1,0}\\ &\quad-(\alpha+\boldsymbol{k}\cdot\boldsymbol{g})T^2\left(1+\frac{2\tau}{T}+\frac{4\tau}{\pi T}\right),\end{aligned} \quad (30)$$

which is consistent with the previous works.[63–65,67] For different definitions for the time T, the final phase shift can be retrieved consistently. For example, when $\tilde{T}$ is defined as the time in between the centers of two consecutive Raman pulses, the consistent result can be derived through a replacement of $\tilde{T}=T+\tau_1/2+\tau_2/2$. In this paper, we focus on the interference phase shift $\Delta\varphi_B$. For convenience, we decompose $\Delta\varphi_B$ into three parts: the atomic free propagation phase shit $\Delta\varphi_{B,\mathrm{prop}}$, the instantaneous interaction phase shift $\Delta\varphi_{B,\mathrm{laser}}$ between the atoms and laser, and the phase shift $\Delta\varphi_{B,\mathrm{obs}}$ related to the position of observation. From Eqs. (24)–(27), these phase shifts can be written as

$$\begin{aligned}\Delta\varphi_{B,\mathrm{prop}} &= 2\frac{\boldsymbol{g}_B}{\hbar}\cdot\left[\left(\boldsymbol{p}+\frac{\hbar\boldsymbol{k}}{2}\right)T^2\left(1+2\frac{\tau}{T}\right)\right.\\ &\quad\left.+m\boldsymbol{g}T^3\left(1+3\frac{\tau}{T}\right)\right],\\ \Delta\varphi_{B,\mathrm{laser}} &= \boldsymbol{k}\cdot\boldsymbol{g}_B\tau^2\left(1-\frac{2}{\pi}\right),\\ \Delta\varphi_{B,\mathrm{obs}} &= \frac{2m\boldsymbol{g}_B\tau}{\hbar}\cdot\boldsymbol{x}.\end{aligned} \quad (31)$$

Usually, we can ignore the phase shift $\Delta\varphi_{B,\mathrm{laser}}$, since it is the high-order effect of τ. Finally, we can derive the total phase as

$$\begin{aligned}\Delta\varphi_B &= 2\frac{m\boldsymbol{g}_B\cdot\boldsymbol{v}_0T^2}{\hbar}\left(1+4\frac{\tau}{T}\right)\\ &\quad+2\frac{m\boldsymbol{g}_B\cdot\boldsymbol{g}T^3}{\hbar}\left(1+5\frac{\tau}{T}\right).\end{aligned} \quad (32)$$

From Eq. (32), we know that $\Delta\varphi_B$ is proportional to the magnetic field gradient $\boldsymbol{g}_B$. To minimize the effect of the magnetic field inhomogeneity and the first-order Zeeman effect, it is necessary to prepare the atoms in the magnetic-field-insensitive states of $m_F=0$. However, the second-order Zeeman effect caused by the weak magnetic field gradient cannot be avoided. To calculate the second-order Zeeman effect, the magnetic field factor $\boldsymbol{g}_B$ should be replaced by Eq. (10), and the related phase shift is

$$\begin{aligned}\Delta\varphi_{B,\mathrm{II}} &= -4\alpha_{Z,\mathrm{II}}B_0\gamma_Be_BT^2(\boldsymbol{v}_0+\boldsymbol{g}T)\\ &\quad-4\alpha_{Z,\mathrm{II}}B_0\gamma_Be_BT\tau(4\boldsymbol{v}_0+5\boldsymbol{g}T).\end{aligned} \quad (33)$$

Apparently, the phase shift related to the magnetic field gradient can be divided into two parts: the pulse-duration-independence part and the pulse-duration-dependence part. The former is the main term and wholly agreed with the previous analysis,[27] which shows that the phase shift related to the magnetic field gradient can be further reduced with a symmetrical interferometer. The latter we are concerned with is tiny, and can be written as

$$\Delta\varphi_{B,\mathrm{II}\tau}=-4\alpha_{Z,\mathrm{II}}B_0\gamma_Be_BT\tau(4\boldsymbol{v}_0+5\boldsymbol{g}T), \quad (34)$$

which has not been studied before. From this equation, the coupling effect of the pulse-duration τ and the magnetic field gradient γ_B is also related to the initial atomic velocity. As the pulse-duration-dependence part contributes a smaller systematic error than the pulse-duration-independence part, it is very urgent to minimize the effect of the magnetic field gradient, which usually requires the well-controlled magnetic fields and extensive magnetic shielding. Based on the typical experimental parameters

$$\begin{aligned}&\alpha_{Z,\mathrm{II}}=2\pi\times575.15\ \mathrm{Hz/G^2},\\ &B_0=0.03\ \mathrm{G},\quad \gamma_B=0.05\ \mathrm{G/m},\\ &T=0.2\ \mathrm{s},\quad \tau=4\times10^{-5}\ \mathrm{s},\\ &v_0=1.95\ \mathrm{m/s},\quad g=-9.8\ \mathrm{m/s^2},\end{aligned} \quad (35)$$

we can reasonably evaluate these effects, the pulse-duration-dependence effect is about $5.5\times10^{-11}g$, which is about thirty times smaller than the pulse-duration-independence effect. When further increasing the magnetic field gradient and pulse duration, the pulse-duration-dependence effect becomes more prominent. We believe that the pulse-duration effect related to the magnetic field gradient plays an important role when one estimates a high-precision atom interferometer, such as the accuracy of $10^{-10}g$. This effect may also be paid more attention to in the high-precision measurements of gravity gradient,[8–10] the fine structure constant,[11–13] the Sagnac effect,[14–16] and the Newtonian gravitational constant.[17,18]

4. Discussion

Usually, the $\boldsymbol{k}_{\mathrm{eff}}$-vector reversal technique is adopted in the gravity measurements, since this technique can well reject some effects independent of the direction of the Raman-pulse wavevector, such as the second-order Zeeman effect and AC Stark effect. Here we just consider the second-order Zeeman effect in gravity measurements. With the $\boldsymbol{k}_{\mathrm{eff}}$-vector reversal technique, the phase shift related to the second-order Zeeman effect can be mostly suppressed, but cannot be canceled completely due to the spatial nonoverlap in the two configurations.

The phase shift of an atom interferometer in two configurations of the $\boldsymbol{k}_{\rm eff}$-vector reversal technique can be expressed as

$$\begin{aligned}\Delta\Phi_{+\boldsymbol{k}_{\rm eff}} &= k_{\rm eff}gT^2+\Delta\varphi_{B,{\rm II},+\boldsymbol{k}_{\rm eff}},\\ \Delta\Phi_{-\boldsymbol{k}_{\rm eff}} &= -k_{\rm eff}gT^2+\Delta\varphi_{B,{\rm II},-\boldsymbol{k}_{\rm eff}},\end{aligned}\tag{36}$$

with $\Delta\varphi_{B,{\rm II},+\boldsymbol{k}_{\rm eff}}$ and $\Delta\varphi_{B,{\rm II},-\boldsymbol{k}_{\rm eff}}$ respectively the phase shifts related to the second-order Zeeman effects in the $+\boldsymbol{k}_{\rm eff}$ and $-\boldsymbol{k}_{\rm eff}$ configurations, which can be written as

$$\begin{aligned}\Delta\varphi_{B,{\rm II},+\boldsymbol{k}_{\rm eff}} &= 2\frac{m\boldsymbol{g}_{B,{\rm II}}\cdot(\boldsymbol{v}_0+\boldsymbol{v}_{\rm r})T^2}{\hbar}\Big(1+4\frac{\tau}{T}\Big)\\ &\quad+2\frac{m\boldsymbol{g}_{B,{\rm II}}\cdot\boldsymbol{g}T^3}{\hbar}\Big(1+5\frac{\tau}{T}\Big),\\ \Delta\varphi_{B,{\rm II},-\boldsymbol{k}_{\rm eff}} &= 2\frac{m\boldsymbol{g}_{B,{\rm II}}\cdot(\boldsymbol{v}_0-\boldsymbol{v}_{\rm r})T^2}{\hbar}\Big(1+4\frac{\tau}{T}\Big)\\ &\quad+2\frac{m\boldsymbol{g}_{B,{\rm II}}\cdot\boldsymbol{g}T^3}{\hbar}\Big(1+5\frac{\tau}{T}\Big),\end{aligned}\tag{37}$$

where $v_{\rm r}=\hbar\boldsymbol{k}_{\rm eff}/2m$ is the recoil velocity. Then, the differential result only related to the second-order Zeeman effect can be written as

$$\begin{aligned}\Delta\Phi_{B,{\rm diff}} &= (\Delta\varphi_{B,{\rm II},+\boldsymbol{k}_{\rm eff}}-\Delta\varphi_{B,{\rm II},-\boldsymbol{k}_{\rm eff}})/2\\ &= 2\frac{m\boldsymbol{g}_{B,{\rm II}}\boldsymbol{v}_{\rm r}T^2}{\hbar}\Big(1+4\frac{\tau}{T}\Big)\\ &= -4\alpha_{\rm Z,II}B_0\gamma_B e_B\boldsymbol{v}_{\rm r}T^2\Big(1+4\frac{\tau}{T}\Big).\end{aligned}\tag{38}$$

It should be noted that this residual Zeeman phase shift has nothing to do with the symmetry of the atom interferometer, and the rejection results are mainly determined by the magnetic field. With the typical experimental parameters

$$\begin{aligned}&\alpha_{\rm Z,II}=2\pi\times575.15\ {\rm Hz/G^2},\quad B_0=0.03\ {\rm G},\\ &\gamma_B=0.05\ {\rm G/m},\quad T=0.2\ {\rm s},\quad \tau=4\times10^{-5}\ {\rm s},\end{aligned}\tag{39}$$

we estimate the total residual second-order Zeeman effect in differential measurements as $\Delta g_{\Phi_{B,{\rm diff}}}=-8.1\times10^{-10}g$, while the coupling part of the Raman pulse duration and magnetic field gradient is about $\Delta g_{\Phi_{B,\tau,{\rm diff}}}=-6.5\times10^{-13}g$. Although this coupling effect is small, it is necessary to analyze, since it is a non-ignorable effect in the future precision atom interferometers aiming at testing general relativity.

As we know, the atom interferometer has achieved a high sensitivity of $5\times10^{-10}g$ with short integration time,[5] which is a challenging sensitivity for a direct observation. However, a light-pulse atom interferometer for ^{87}Rb with a duration of $2T=2.3$ s has been demonstrated,[37] which inferred the acceleration sensitivity of 6.7×10^{-12} g/shot. In this case, the coupling effect between the Raman-pulse duration and the magnetic field gradient may be easily detected. To achieve a possible observation for the coupling effect of the pulse duration and magnetic field gradient, one can choose the atom interferometer working in a magnetic sensitive sub-level (eg $m_F=+1$). In this configuration, the coupling effect related to the first-order Zeeman effect is calculated as

$$\Delta\varphi_{B,{\rm I},\tau}=-2\alpha_{\rm Z,I}\gamma_B e_B T\tau(4\boldsymbol{v}_0+5\boldsymbol{g}T).\tag{40}$$

From this equation, this coupling effect can be measured by modulating the Raman-pulse duration theoretically. With the typical experimental parameters

$$\alpha_{\rm Z,I}=2\pi\times0.7\ {\rm MHz/G},\quad \gamma_B=0.01\ {\rm G/m},\quad T=25\ {\rm ms},\tag{41}$$

$$\tau=4\times10^{-5}\ {\rm s},\quad \boldsymbol{v}_0=0.23\ {\rm m/s},\quad \boldsymbol{g}=-9.8\ {\rm m/s^2},\tag{42}$$

we can simply estimate this coupling effect as $2.7\times10^{-7}g$, which seems observable experimentally, since the magnetically sensitive interferometer shows a long-term sensitivity better than $1\times10^{-7}g$.[21]

In the real measurement, some other systematic errors should be considered, for example, the AC stark shift. The phase shift due to the AC stark shift is[45]

$$\Delta\phi_{\rm AC}=\left(\frac{\Delta_{\rm ac}^{(3)}}{\Omega_{\rm eff}^{(3)}}-\frac{\Delta_{\rm ac}^{(1)}}{\Omega_{\rm eff}^{(1)}}\right),\tag{43}$$

where $\Delta_{\rm ac}^{(1,3)}$ are the frequency shifts of the Raman transition at the time of the first and the third pulses, and $\Omega_{\rm eff}^{(1,3)}$ are the corresponding effective Rabi frequencies. It must be noted that both $\Delta_{\rm ac}^{(1,3)}$ and $\Omega_{\rm eff}^{(1,3)}$ are proportional to the intensity of the two Raman lasers, which means that there will be no AC stark phase shift contribution by changing the Raman pulse duration, i.e., the AC stark phase shift is just a constant bias. However, the changes of the intensity ratio will lead to the fluctuations of the AC stark shift, which has been estimated at the level of ±1 μGal.[3] Similarly, we can estimate this effect about $3.8\times10^{-8}g$ in our setup.

Therefore, the effect of the Raman-pulse duration related to the magnetic field gradient can be detected with a magnetic sensitive atom interferometer.

5. Conclusion

With a simplified time-propagation operator model, we have calculated the Raman-pulse-duration effect in an inhomogeneous magnetic field for a high-precision atom interferometer, where the coupling effect between the Raman-pulse duration and magnetic field gradient is focused on. Finally, we find that for a typical atom gravimeter, this coupling effect is very tiny, but cannot be ignored when one estimates a higher-precision atom gravimeter, such as the accuracy of $10^{-10}g$. In addition, we have a simple discussion on the possibility of testing this effect.

Appendix A: The time-propagation operator

In order to facilitate the time-propagation operator $U(t)$, we make a unitary transformation with the operator $\hat{O}(t)$,[67,68] and then obtain the transformed Hamiltonian

$$\begin{aligned}\tilde{H} &= \left\{\frac{E_e+E_g}{2}+\frac{\hbar\delta_k}{4}+\frac{\hat{p}^2}{2m}-m\boldsymbol{g}\cdot\boldsymbol{x}\right\}\begin{pmatrix}1&0\\0&1\end{pmatrix}\\ &\quad -m\boldsymbol{g}_B\cdot\boldsymbol{x}\begin{pmatrix}1&0\\0&-1\end{pmatrix}-\frac{\hbar}{2}\hat{\Delta}_0\begin{pmatrix}1&0\\0&-1\end{pmatrix}+\frac{\hbar\Omega}{2}\begin{pmatrix}0&1\\1&0\end{pmatrix}\\ &\equiv H_0+H_B+H_1,\end{aligned} \tag{A1}$$

with

$$\begin{aligned}\tilde{H}_0 &= \left\{\frac{E_e+E_g}{2}+\frac{\hbar\delta_k}{4}+\frac{\hat{p}^2}{2m}-m\boldsymbol{g}\cdot\boldsymbol{x}\right\}\begin{pmatrix}1&0\\0&1\end{pmatrix},\\ \tilde{H}_B &= -m\boldsymbol{g}_B\cdot\boldsymbol{x}\begin{pmatrix}1&0\\0&-1\end{pmatrix},\\ \tilde{H}_1 &= -\frac{\hbar}{2}\hat{\Delta}_0\begin{pmatrix}1&0\\0&-1\end{pmatrix}+\frac{\hbar\Omega}{2}\begin{pmatrix}0&1\\1&0\end{pmatrix},\end{aligned} \tag{A2}$$

where we define the Doppler operator $\hat{D}=\frac{\boldsymbol{k}\cdot\hat{\boldsymbol{p}}}{m}$, the recoil shift $\delta_k=\frac{\hbar\boldsymbol{k}^2}{2m}$, and the Raman detuning $\hat{\Delta}_0=\omega_{\mathrm{L}}-\omega_{eg}-\hat{D}$. By using the unitary transformation with $\hat{O}(t)$, the new propagation operator $\tilde{U}(t)$ is given by

$$\tilde{U}(t)=\hat{O}(t)U(t)\hat{O}^{-1}(0)=\mathrm{e}^{-\mathrm{i}t\tilde{H}/\hbar}. \tag{A3}$$

To separate the center-of-mass motion from $\tilde{H}$, we rewrite $\tilde{U}(t)$ as

$$\tilde{U}(t)=\mathrm{e}^{-\mathrm{i}t(H_0+H_B)/\hbar}W(t). \tag{A4}$$

According to the Schrödinger equation, the dynamic equation for $W(t)$ can be express as

$$\begin{aligned}\mathrm{i}\hbar\dot{W}(t) &= \mathrm{e}^{\mathrm{i}t(H_0+H_B)/\hbar}H_1\,\mathrm{e}^{-\mathrm{i}t(H_0+H_B)/\hbar}W(t)\\ &= \left[-\frac{\hbar}{2}\hat{\Delta}_t\sigma_3+\frac{\hbar\Omega}{2}\sigma_1+\frac{\hbar}{2}\boldsymbol{k}\cdot\boldsymbol{g}_B t\right.\\ &\quad \left.-m\boldsymbol{g}_B\cdot\boldsymbol{x}\Omega t\sigma_2\right]W(t),\end{aligned} \tag{A5}$$

where $\sigma_1,\sigma_2,\sigma_3$ are the Pauli matrices, $\hat{\Delta}_t=\omega_{\mathrm{L}}-\omega_{eg}-\hat{D}-\boldsymbol{k}\cdot\boldsymbol{g}t$. Considering the frequency-sweeping rate α, we rewrite $\hat{\Delta}_t$ as

$$\hat{\Delta}_t=\omega_{\mathrm{L}}-\omega_{eg}-\hat{D}-(\alpha+\boldsymbol{k}\cdot\boldsymbol{g})t. \tag{A6}$$

For simplicity, we define

$$W(t)=\exp\left[-\frac{\mathrm{i}t^2}{4}\boldsymbol{k}\cdot\boldsymbol{g}_B+\frac{\mathrm{i}t^2m\boldsymbol{g}_B\cdot\boldsymbol{x}\Omega}{2}\sigma_2\right]Y(t), \tag{A7}$$

Based on Eq. (A5), we obtain

$$\mathrm{i}\hbar\dot{Y}(t)=\left[-\frac{\hbar}{2}\hat{\Delta}_0\sigma_3+\frac{\hbar\Omega}{2}\sigma_1\right]Y(t), \tag{A8}$$

and further obtain

$$\begin{aligned}Y(t) &= \mathrm{e}^{-\mathrm{i}tH_1/\hbar}\\ &= \exp\left[\frac{\mathrm{i}t}{2}(\hat{\Delta}_0\sigma_3-\Omega\sigma_1)\right]\\ &= \begin{bmatrix}\cos\frac{\hat{\omega}t}{2}+\mathrm{i}\frac{\hat{\Delta}_0}{\hat{\omega}}\sin\frac{\hat{\omega}t}{2} & -\mathrm{i}\frac{\Omega}{\hat{\omega}}\sin\frac{\hat{\omega}t}{2}\\ -\mathrm{i}\frac{\Omega}{\hat{\omega}}\sin\frac{\hat{\omega}t}{2} & \cos\frac{\hat{\omega}\tau}{2}-\mathrm{i}\frac{\hat{\Delta}_0}{\hat{\omega}}\sin\frac{\hat{\omega}t}{2}\end{bmatrix},\end{aligned} \tag{A9}$$

where $\hat{\omega}=\sqrt{\Omega^2+\Delta_0^2}$. Combining Eqs. (A4) and (A7), we can derive

$$\begin{aligned}\tilde{U}(t) &= \exp\left[-\mathrm{i}\left(\frac{\omega_e+\omega_g}{2}+\frac{\delta_k}{4}+\frac{\hat{p}^2}{2m\hbar}\right.\right.\\ &\quad \left.\left.-\frac{m\boldsymbol{g}\cdot\boldsymbol{x}}{\hbar}-\frac{m\boldsymbol{g}_B\cdot\boldsymbol{x}}{\hbar}\sigma_3\right)t\right]\\ &\quad \times\exp\left[-\frac{\mathrm{i}t^2}{4}\boldsymbol{k}\cdot\boldsymbol{g}_B+\frac{\mathrm{i}t^2m\boldsymbol{g}_B\cdot\boldsymbol{x}\Omega}{2}\sigma_2\right]Y(t).\end{aligned} \tag{A10}$$

Finally, $U(t)$ can be given by

$$\begin{aligned}U(t) &= \exp\left[-\mathrm{i}\left(\frac{\omega_e+\omega_g}{2}+\frac{\delta_k}{2}+\frac{\hat{p}^2}{2m\hbar}-\frac{m\boldsymbol{g}\cdot\boldsymbol{x}}{\hbar}-\frac{m\boldsymbol{g}_B\cdot\boldsymbol{x}}{\hbar}\sigma_3\right)t\right]\begin{pmatrix}\mathrm{e}^{-\mathrm{i}\frac{\omega_{\mathrm{L}}t-\hat{D}t}{2}}\mathrm{e}^{\mathrm{i}\frac{(\alpha+\boldsymbol{k}\cdot\boldsymbol{g})t^2}{4}} & 0\\ 0 & \mathrm{e}^{\mathrm{i}\frac{\omega_{\mathrm{L}}t-\hat{D}t}{2}}\mathrm{e}^{-\mathrm{i}\frac{(\alpha+\boldsymbol{k}\cdot\boldsymbol{g})t^2}{4}}\end{pmatrix}\\ &\quad \times\exp\left[\frac{\mathrm{i}t^2m\boldsymbol{g}_B\cdot\boldsymbol{x}\Omega}{2}\sigma_2\right]\begin{bmatrix}Y_{11}(\boldsymbol{p}_-) & Y_{12}(\boldsymbol{p}_-)\mathrm{e}^{\mathrm{i}(\boldsymbol{k}\cdot\boldsymbol{x}-\phi_{\mathrm{L},0})}\\ Y_{21}(\boldsymbol{p}_+)\mathrm{e}^{-\mathrm{i}(\boldsymbol{k}\cdot\boldsymbol{x}-\phi_{\mathrm{L},0})} & Y_{22}(\boldsymbol{p}_+)\end{bmatrix},\end{aligned} \tag{A11}$$

with Y_{ij} the matrix elements. Here to abbreviate the momentum, we introduce $\boldsymbol{p}_+=\boldsymbol{p}+\hbar\boldsymbol{k}/2$ and $\boldsymbol{p}_-=\boldsymbol{p}-\hbar\boldsymbol{k}/2$. α is the frequency-sweeping rate, which is used to compensate the first-order Doppler shift of the freely falling atoms in the experiments, and $\alpha\approx-\boldsymbol{k}\cdot\boldsymbol{g}$. Thus, equation (A11) can be further simplified as

$$\begin{aligned}U(t) &= \begin{pmatrix}\mathrm{e}^{-\mathrm{i}\beta_e t}&0\\0&\mathrm{e}^{-\mathrm{i}\beta_g t}\end{pmatrix}\begin{pmatrix}\mathrm{e}^{-\mathrm{i}\eta_1(t)}&0\\0&\mathrm{e}^{\mathrm{i}\eta_2(t)}\end{pmatrix}\\ &\quad \times\begin{pmatrix}Y_{11}(\boldsymbol{p}_-) & Y_{12}(\boldsymbol{p}_-)\mathrm{e}^{\mathrm{i}\lambda}\\ Y_{21}(\boldsymbol{p}_+)\mathrm{e}^{-\mathrm{i}\lambda} & Y_{22}(\boldsymbol{p}_+)\end{pmatrix},\end{aligned} \tag{A12}$$

here, we have ignored the quadratic terms of time t, and defined

$$\beta_e = \omega_e + \frac{\hat{p}^2}{2m\hbar} - \frac{m(\boldsymbol{g}+\boldsymbol{g}_B)\cdot\boldsymbol{x}}{\hbar},$$
$$\beta_g = \omega_g + \frac{\hat{p}^2}{2m\hbar} - \frac{m(\boldsymbol{g}-\boldsymbol{g}_B)\cdot\boldsymbol{x}}{\hbar},$$
$$\eta_1(t) = (\omega_{\rm L} - \omega_{eg} - \hat{D} + \delta_k)t/2,$$
$$\eta_2(t) = (\omega_{\rm L} - \omega_{eg} - \hat{D} - \delta_k)t/2,$$
$$\delta_0 = \omega_{\rm L} - \omega_{eg} - \boldsymbol{k}\cdot\hat{\boldsymbol{p}}/m - h\boldsymbol{k}^2/2m,$$
$$\lambda = \boldsymbol{k}\cdot\boldsymbol{x} - \phi_{\rm L,0}. \tag{A13}$$

$$Y_{11}(\boldsymbol{p}) = \cos\frac{\theta}{2} + {\rm i}\frac{2\delta_0 t - (\alpha+\boldsymbol{k}\cdot\boldsymbol{g})t^2}{4}\frac{\sin\theta/2}{\theta/2},$$
$$Y_{12}(\boldsymbol{p}) = -{\rm i}\sin\frac{\theta}{2} + \frac{(\alpha+\boldsymbol{k}\cdot\boldsymbol{g})t^2}{2\theta}\left(\cos\frac{\theta}{2} - \frac{\sin\theta/2}{\theta/2}\right),$$
$$Y_{21}(\boldsymbol{p}) = -{\rm i}\sin\frac{\theta}{2} + \frac{(\alpha+\boldsymbol{k}\cdot\boldsymbol{g})t^2}{2\theta}\left(\cos\frac{\theta}{2} - \frac{\sin\theta/2}{\theta/2}\right),$$
$$Y_{22}(\boldsymbol{p}) = \cos\frac{\theta}{2} - {\rm i}\frac{2\delta_0 t - (\alpha+\boldsymbol{k}\cdot\boldsymbol{g})t^2}{4}\frac{\sin\theta/2}{\theta/2}. \tag{A14}$$

References

[1] Kasevich M and Chu S 1991 *Phys. Rev. Lett.* **67** 181

[2] Wang J 2015 *Chin. Phys. B* **24** 053702

[3] Peters A, Chung K Y and Chu S 2001 *Metrologia* **38** 25

[4] Louchet-Chauvet A, Farah T, Bodart Q, Clairon A, Landragin A, Merlet S and Pereira Dos Santos F 2011 *New J. Phys.* **13** 065025

[5] Hu Z K, Sun B L, Duan X C, Zhou M K, Chen L L, Zhan S, Zhang Q Z and Luo J 2013 *Phys. Rev. A* **88** 043610

[6] Freier C, Hauth M, Schkolnik V, Leykauf B, Schilling M, Wziontek H, Scherneck H G, Müller J and Peters A 2016 *J. Phys.: Conf. Ser.* **723** 012050

[7] Zhou M K, Duan X C, Chen L L, Luo Q, Xu Y Y and Hu Z K 2015 *Chin. Phys. B* **24** 050401

[8] D'Amico G, Borselli F, Cacciapuoti L, Prevedelli M, Rosi G, Sorrentino F and Tino G M 2016 *Phys. Rev. A* **93** 063628

[9] Sorrentino F, Bertoldi A, Bodart Q, Cacciapuoti L, de Angelis M, Lien Y H, Prevedelli M, Rosi G and Tino G M 2012 *Appl. Phys. Lett.* **101** 114106

[10] Snadden M J, McGuirk J M, Bouyer P, Haritos K G and Kasevich M A 1998 *Phys. Rev. Lett.* **81** 971

[11] Bouchendira R, Cladé P, Guellati-Khélifa S, Nez F and Biraben F 2011 *Phys. Rev. Lett.* **106** 080801

[12] Bouchendira R, Cladé P, Guellati-Khélifa S, Nez F and Biraben F 2013 *Ann. Phys.* (Berlin) **525** 484

[13] Estey B, Yu C H, Kuan P C, Lan S Y and Müller H 2015 *Phys. Rev. Lett.* **115** 083002

[14] Dutta I, Savoie D, Fang B, Venon B, Garrido Alzar C L, Geiger R and Landragin A 2016 *Phys. Rev. Lett.* **116** 183003

[15] Yao Z W, Lu S B, Li R B, Wang K, Cao L, Wang J and Zhan M S 2016 *Chin. Phys. Lett.* **33** 083701

[16] Gustavson T L, Landragin A and Kasevich M A 2000 *Class. Quantum Grav.* **17** 2385

[17] Lamporesi G, Bertoldi A, Cacciapuoti L, Prevedelli M and Tino G M 2008 *Phys. Rev. Lett.* **100** 050801

[18] Rosi G, Sorrentino F, Cacciapuoti L, Prevedelli M and Tino G M 2014 *Nature* **510** 518

[19] Fray S, Diez C A, Hänsch T W and Weitz M 2004 *Phys. Rev. Lett.* **93** 240404

[20] Zhou L, Long S T, Tang B, Chen X, Gao F, Peng W C, Duan W T, Zhong J Q, Xiong Z Y, Wang J, Zhang Y Z and Zhan M S 2015 *Phys. Rev. Lett.* **115** 013004

[21] Duan X C, Deng X B, Zhou M K, Zhang K, Xu W J, Xiong F, Xu Y Y, Shao C G, Luo J and Hu Z K 2016 *Phys. Rev. Lett.* **117** 023001

[22] Rosi G, D'Amico G, Cacciapuoti L, Sorrentino F, Prevedelli M, Zych M, Brukner Č and Tino G M 2017 *Nat. Commun.* **8** 15529

[23] Aguilera D, Ahlers H, Battelier B *et al.* 2014 *Class. Quantum Grav.* **31** 115010

[24] Chiow S W, Williams J, Yu N and Müller H 2017 *Phys. Rev. A* **95** 021603(R)

[25] Dimopoulos S, Graham P W, Hogan J M, Kasevich M A and Rajendran S 2009 *Phys. Lett. B* **678** 37

[26] Graham P W, Hogan J M, Kasevich M A, Rajendran S and Romani R W arXiv:1711.02225v1

[27] Zhou M K, Hu Z K, Duan X C, Sun B L, Zhao J B and Luo J 2010 *Phys. Rev. A* **82** 061602(R)

[28] Hu Z K, Duan X C, Zhou M K, Sun B L, Zhao J B, Huang M M and Luo J 2011 *Phys. Rev. A* **84** 013620

[29] Wu B, Wang Z Y, Cheng B, Wang Q Y, Xu A P and Lin Q 2014 *J. Phys. B: At. Mol. Opt. Phys.* **47** 015001

[30] Li R B, Zhou L, Wang J and Zhan M S 2009 *Opt. Commun.* **282** 1340

[31] Bordé C J 1989 *Phys. Lett. A* **140** 10

[32] Giltner D M, McGowan R W and Lee S A 1995 *Phys. Rev. A* **52** 3966

[33] Chiow S W, Kovachy T, Chien H C and Kasevich M A 2011 *Phys. Rev. Lett.* **107** 130403

[34] Müller H, Chiow S W, Long Q, Herrmann S and Chu S 2008 *Phys. Rev. Lett.* **100** 180405

[35] Altin P A, Johnsson M T, Negnevitsky V, Dennis G R, Anderson R P, Debs J E, Szigeti S S, Hardman K S, Bennetts S, McDonald G D, Turner L D, Close J D and Robins N P 2013 *New J. Phys.* **15** 023009

[36] Cheng Y, Zhang K, Chen L L, Xu W J, Luo Q, Zhou M K and Hu Z K 2017 *AIP Advances* **7** 095211

[37] Dickerson S M, Hogan J M, Sugarbaker A, Johnson D M S and Kasevich M A 2013 *Phys. Rev. Lett.* **111** 083001

[38] Zhou L, Xiong Z Y, Yang W, Tang B, Peng W C, Hao K, Li R B, Liu M, Wang J and Zhan M S 2011 *Gen. Relativ. Gravit.* **43** 1931

[39] Zhang X, Del Aguila R, Mazzoni T, Poli N and Tino G M 2016 *Phys. Rev. A* **94** 043608

[40] Kovachy T, Asenbaum P, Overstreet C, Donnelly C A, Dickerson S M, Sugarbaker A, Hogan J M and Kasevich M A 2015 *Nature* **528** 530

[41] Novak P 2010 *Surv. Geophys.* **31** 1

[42] Fang J C and Qin J 2012 *Sensors* **12** 6331

[43] Rosi G, Cacciapuoti L, Sorrentino F, Menchetti M, Prevedelli M and Tino G M 2015 *Phys. Rev. Lett.* **114** 013001

[44] Duan X C, Mao D K, Deng X B, Zhou M K, Shao C G, Zhu Z and Hu Z K 2018 *Chin. Phys. B* **27** 013701

[45] Gauguet A, Canuel B, Lévèque T, Chaibi W and Landragin A 2009 *Phys. Rev. A* **80** 063604

[46] Wu J Z, Ji Z K, Zhang Y C, Wang L R, Zhao Y Y, Ma J, Xiao L T and Jia S T 2011 *Opt. Lett.* **36** 2038

[47] Zhang Y C, Ma J, Li Y Q, Wu J Z, Zhang L J, Chen G, Zhao Y Y, Xiao L T and Jia S T 2012 *Appl. Phys. Lett.* **101** 131114

[48] Zhou M K, Chen L L, Luo Q, Zhang K, Duan X C and Hu Z K 2016 *Phys. Rev. A* **93** 053615

[49] Hu Q Q, Freier C, Leykauf B, Schkolnik V, Yang J, Krutzik M and Peters A 2017 *Phys. Rev. A* **96** 033414

[50] Cheng B, Wang Z Y, Xu A P, Wang Q Y and Lin Q 2015 *Chin. Phys. B* **24** 013704

[51] Goüet J L, Mehlsťaubler T, Kimb J, Merlet S, Clairon A, Landragin A and Pereira Dos Santos F 2008 *Appl. Phys. B* **92** 133

[52] Wu B, Wang Z Y, Cheng B, Wang Q Y, Xu A P and Lin Q 2014 *Metrologia* **51** 452

[53] Deng X B, Duan X C, Mao D K, Zhou M K, Shao C G and Hu Z K 2017 *Chin. Phys. B* **26** 043702

[54] Wolf P and Tourrenc P 1999 *Phys. Lett. A* **251** 241

[55] Gauguet A, Mehlstäubler T E, Lévèque T, Le Gouët J, Chaibi W, Canuel B, Clairon A, Pereira Dos Santos F and Landragin A 2008 *Phys. Rev. A* **78** 043615

[56] Schkolnik V, Leykauf B, Hauth M, Freier C and Peters A 2015 *Appl. Phys. B* **120** 311

[57] Zhou M K, Luo Q, Chen L L, Duan X C and Hu Z K 2016 *Phys. Rev. A* **93** 043610

[58] Trimeche A, Langlois M, Merlet S and Pereira Dos Santos F 2017 *Phys. Rev. Appl.* **7** 034016
[59] Lan S Y, Kuan P C, Estey B, Haslinger P and Müller H 2012 *Phys. Rev. Lett.* **108** 090402
[60] Le Goüet J, Cheinet P, Kimb J, Holleville D, Clairon A, Landragin A and Pereira Dos Santos F 2007 *Eur. Phys. J. D* **44** 419
[61] Cheng B, Gillot P, Merlet S and Pereira Dos Santos F 2015 *Phys. Rev. A* **92** 063617
[62] Tan Y J, Shao C G and Hu Z K 2017 *Phys. Rev. A* **96** 023604
[63] Peters A 1998 *High Precision Gravity Measurements Using Atom Interferometry* (Ph.D. thesis) (Stanford University)
[64] Butts D L, Kinast J M, Timmons B P and Stoner R E 2011 *J. Opt. Soc. Am. B* **28** 3
[65] Stoner R, Butts D, Kinast J and Timmons B 2011 *J. Opt. Soc. Am. B* **28** 10
[66] Shao C G, Mao D K, Zhou M K, Tan Y J, Chen L L, Luo J and Hu Z K 2015 *Phys. Rev. A* **92** 053613
[67] Li X, Shao C G and Hu Z K 2015 *J. Opt. Soc. Am. B* **32** 2
[68] Marzlin K P and Audretsch J 1996 *Phys. Rev. A* **53** 2
[69] Steck D A http://steck.us/alkalidata/rubidium87numbers.1.6.pdf